PNAS
www.pnas.org

Supplementary information for

Distinct locomotor precursors in newborn babies

Francesca Sylos-Labini, Valentina La Scaleia, Germana Cappellini, Adele Fabiano, Simonetta Picone, Elena S. Keshishian, Dmitry S. Zhvansky, Piermichele Paolillo, Irina A. Solopova, Andrea d'Avella, Yury Ivanenko, Francesco Lacquaniti

This PDF file includes: Supplementary Methods, Figures S1 to S6

Supplementary Methods

Participants

All experiments were in accordance with the World Medical Association Declaration of Helsinki for medical research involving human subjects. The experiments were approved by the Research Ethics Committees of Azienda Sanitaria Locale (Local Health Centre) Roma C (protocol CEI/15843 study n. 609, and protocol 27593, study n. 38.15), Santa Lucia Foundation (protocol CE/AG4/PROG.341-01), and Veltischev Research and Clinical Institute for Pediatrics of the Pirogov Russian National Research Medical University (protocol n. 14/18). A parent for the child and all adult subjects provided informed written consent to participate in the study after the nature and possible consequences of the study were explained. All children were full-term at birth and had no known pathology. The sample of recorded children included neonates (n=84, median age 2 days postpartum, interquartile range 3 days, 46 males and 38 females, Apgar score ≥8 at 1 and 5 min, uneventful delivery and perinatal history) and children of 6 different age groups (for a total of n=77, 46 males and 31 females): group 1 (g1, n=21, age range 4-6 months), group 2 (g2, n=12, 6-8 months), group 3 (g3, n=8, 8-10 months), group 4 (g4, n=11, 10-14 months), group 5 (g5, toddlers n=17, 12-15 months), and group 6 (g6, preschoolers n=8, 24-48 months). Neonates and g1-g4 infants were unable to perform unsupported stepping, while g5 and g6 children walked unsupported. Toddlers (g5) were recorded within 4 weeks from the first day of unsupported walking experience (as reported by the parent). Since it was not possible to perform all tests and recordings on all children for clinical reasons or lack of compliance, in the main text and the supplementary material we specify the number of participants for each test and analysis. Healthy adults (n=16, 27 ± 6 years, mean ± SD, 13 males and 3 females) served as a reference. De-identified data from the participants were used in all analyses and Figures.

Experimental protocols

NEONATES. Neonates were studied in the hospital well-baby maternity ward. Stepping was elicited following established procedures (1-7). An experienced pediatrician held the child under the armpits, with the feet soles touching a flat surface. Stepping was typically successful when the child was sufficiently aroused. No movement recording was carried out if the child was drowsy or asleep. We studied stepping in two groups of neonates with different experimental protocols.

Neonates of the first group (n=33) stepped on a horizontal walkway. In each trial, the neonate was gently pulled forwards along the walkway, being raised and repositioned at the start of the walkway each time.

A second group of neonates (n=21) stepped on a treadmill at different speeds and directions. Each experiment started with stepping trials at 0.03 m/s. All these neonates were then tested at 0.05 and 0.1 m/s. Higher speeds (0.15, 0.2 m/s) were tested only if the neonate was able to step at a lower speed. The belt speed was generally changed between the trials (with the child not in contact with the treadmill). Occasionally, the belt speed was changed in mid-trial; in these instances, the steps performed during the acceleration or deceleration phase were not included in the analysis. In 11 neonates of this group, we also tested stepping with the child placed supine in a horizontal position, while the treadmill was oriented perpendicular to the ground. In this protocol, the neonate was

supported on the back by the pediatrician and was gently pushed horizontally in contact with the treadmill. Belt speed was set at 0.05 m/s.
We recorded spontaneous kicking movements in 35 neonates following established procedures (4-5). In 18 neonates, kicking was recorded while they were placed supine on a table covered by a disposable pad. In 10 of these neonates, kicking was recorded on the same occasion as stepping, either just before or just afterwards. In 17 neonates (different from the previous ones), kicking was recorded while they were held under the armpits vertically in air by the pediatrician.

INFANTS, TODDLERS AND PRESCHOOLERS. They were studied in a hospital laboratory or pediatric room. Thirty-eight children (from groups g1-g5) were tested on a treadmill with incremental speeds in the range between 0.05 m/s and 0.6 m/s. Thirty-nine children (from groups g1-g6) were tested on a horizontal walkway. All infants younger than 8 months had not practiced stepping before the recording sessions, except one infant (6.7 months) who once experienced stepping on treadmill in the laboratory about 3 months earlier. In infants unable to step unsupported (g1-g4), stepping was elicited in a manner similar to that used for neonates. For the toddlers (g5), one parent initially held the child by hand, then she or he parent started moving forward, leaving the child's hand and encouraging her or him to walk unsupported on the floor. Both a parent and an experimenter remained astride to prevent falls. Preschoolers (g6) walked naturally at their preferred speed.

ADULTS. They walked at 1.1 m/s (4 km/h) on a treadmill.

Experimental setups and recordings
Neonates of the first group stepped on the Walkway Tekscan (Tekscan Inc, South Boston, USA, 95 cm x 44 cm, length x width, 4 sensors/cm^2, factory-calibrated for the low pressure values), which recorded the vertical load distribution underneath the plantar surface of the feet at 50 samples/s. Neonates of the second group, children (except those who stepped on a horizontal walkway) and adults stepped on a pediatric treadmill model 2 Carlin's Creations (Sturgis, MI, 69 cm x 46 cm length x width), model 3 Carlin's Creations (Sturgis, MI, 81 cm x 46 cm), and standard treadmill (EN-Mill 3446.527, Bonte Zwolle BV, BO Systems, The Netherlands, 150 x 60 cm), respectively.
Kinematics was recorded by means of a video camera (Canon MD160, Canon Inc., Japan, 1152 x 864 pixels, 25 frames/s or Panasonic HC-V760EE-K, 1920 x 1080 pixels, 50 frames/s) for children who stepped on a walkway. We used a 3D SIMI motion capture system (Munich, Germany, 3 video cameras, 640 x 480 pixels, 100 frames/s) to record kicking and stepping on treadmill in neonates, and a 3D Vicon Nexus (Oxford, UK, 10 Bonita cameras, 1024 x 1024 pixels, 200 frames/s) in children who stepped on treadmill and adults. In all cases, adhesive markers (diameter, 9 and 14 mm in neonates and older participants, respectively) were attached to the skin over the hip (greater trochanter, GT), knee (lateral femur epicondyle, LE), ankle (lateral malleolus, LM), and fifth metatarsophalangeal joint (5MT) of the leg facing the video cameras.
In neonates, surface EMG activities were recorded at 2 kHz using the wireless Zerowire system (Aurion Srl, Italy) with miniature (2-mm diameter) surface electrodes (Beckman Instruments), bandwidth of 20–1000 Hz with an overall gain of 1000. To minimize movement artifacts,

preamplified EMG sensor units were attached at the experimenter's wrist, and twisted pairs of wires (between electrodes and units) were limited to 25 cm length and fixed along the neonate's leg using elastic gauze (1-3). In children and adults, EMGs were recorded by means of the Trigno Wireless EMG System (Delsys Inc., Boston, MA, bar electrodes, contact 5 x 1 mm), bandwidth of 20–450 Hz, overall gain of 1000. Sampling rate was 2 kHz for participants stepping on treadmill, and 963 Hz for those stepping on a horizontal walkway. In all neonates and all other children, we recorded bilaterally from rectus femoris (RF), biceps femoris (BF), tibialis anterior (TA), and gastrocnemius lateralis (LG). In 10 neonates, we also recorded bilaterally from gluteus maximus (GM), tensor fascia latae (TFL), adductor longus (Add), vastus lateralis (VL), vastus medialis (VM), gastrocnemius medialis (MG), and soleus (Sol). In all adults, we recorded bilaterally from gluteus medius (Gmed), tensor fascia latae (TFL), semitendinosus (ST), biceps femoris (BF), rectus femoris (RF), vastus lateralis (VL), vastus medialis (VM), gastrocnemius medialis (MG), gastrocnemius lateralis (LG), soleus (Sol), and tibialis anterior (TA). In all experiments, sampling of kinematic and EMG data was synchronized. All markers and electrodes used in children were for pediatric use.

Data analysis

Kinematics

The acquired kinematic data were low pass filtered at 20 Hz with a zero-lag Butterworth filter. The principal plane of movement was the subject's sagittal plane for stepping. For spontaneous movements, the principal movement plane was defined by the average positions (across all flexion-extension units of a given trial, see below) of GT, LE and LM markers. The spatial reference system for spontaneous movements was aligned with this plane: y-axis aligned with the average LM-GT direction, x-axis perpendicular to y-axis in the plane, z-axis normal to the plane. The instantaneous distance between GT and LM markers defined the effective limb length, denoting the variable extent of flexion-extension. Tangential (3D) foot velocity was computed as $\sqrt{(\dot{x}^2 + \dot{y}^2 + \dot{z}^2)}$, using the instantaneous coordinates of 5MT.

For stepping, we selected the sequences with at least 3 consecutive steps involving alternating (left-right) foot placements. Stance and swing phases were defined on the basis of the timing of the local minima of the vertical position of the foot markers (LM and 5MT), and contact force recordings when available. Stride cycle was defined as the time interval between two successive touch-downs by the same foot, and included a step of one foot followed by a step of the contralateral foot. A step was defined as a cyclic movement that included the placement of 5MT ahead of GT. The kinematic data were time-interpolated over individual step cycles to fit a normalized 200-point time base. They were averaged across all strides only for analysis of ensemble data.

For kicking, we defined a FEU as a segment of spontaneous movements that consisted of a leg flexion followed by leg extension, according to the following procedure (Fig. S3). We computed the maximum value of effective limb length over the whole trial. The minima of limb lengths that were at least 2 cm smaller than the maximum limb length were used to define a FEU. To detect its onset and end, we identified the maxima of limb length between two consecutive minima. We selected only FEUs in which the peak of foot velocity exceeded a threshold of 0.2 m/s.

Spontaneous movements data were time-interpolated over individual FEUs to fit a normalized 200-points time base and averaged across FEUs.

EMG activity

Raw digitized EMG data were first inspected visually to detect artifacts and remove the corrupted data segment from further analysis. Because of the low skin impedance at each electrode site and the preamplification close to the electrodes, artifacts were infrequent (less than 4% of recorded data were removed). EMG data were high-pass filtered at 60 Hz, full-wave rectified, and low-pass-filtered at 3 Hz (5 Hz in the adults) to obtain envelope time-series. All filters were zero-lag 4^{th}-order Butterworth. For spontaneous movements, in order to evaluate the EMG activity preceding each FEU, an interval of the same duration as that of the FEU was considered before each FEU onset. Similarly to the kinematic data, also the processed EMG data were time-interpolated over a normalized 200-point time base, and were averaged across all cycles only for analysis of ensemble data.

For each muscle, we calculated the center-of-activity (CoA) over a step cycle or over -100%÷100% FEU to assess if the temporal modulation of activity was consistent across cycles. We chose to analyze CoAs because single peaks of activity could not be identified reliably in the majority of cases. The CoA during each cycle was calculated using circular statistics (circ_moment.m function in the CircStat Matlab toolbox, 8), and the distribution of CoA across cycles was plotted with polar histograms. Polar direction denotes the phase of the movement cycle (with angle θ that varies from 0 to 360° corresponding to 0 and 100% cycle for stepping, and to -100% and 100% FEU for spontaneous movements), and the height of each bar in the polar histogram indicates the percentage of steps or kicks in which the CoA of the muscle is located within a given sector. The CoA of the EMG waveform was calculated as the angle of the vector (first trigonometric moment) pointing to the center of mass of the circular distribution:

$$A = \sum_{t=1}^{200}(\cos\theta_t \times EMG_t) \quad (1)$$

$$B = \sum_{t=1}^{200}(\sin\theta_t \times EMG_t) \quad (2)$$

$$CoA = \tan^{-1}(B/A) \quad (3)$$

The CoA was considered only for those cycle in which the EMG waveform was not uniformly distributed along the movement cycle (Rayleigh test for non-uniformity of circular data $P<0.05$).

Basic neuromuscular modules of bilateral EMGs

Processed EMG signals were first segmented over a step cycle or -100%÷100% FEU. Basic neuromuscular modules were extracted from bilateral EMG time-varying profiles of each single cycle for all participants using the non-negative matrix factorization (NNMF) algorithm (9). Before applying NNMF, we subtracted the minimum over the cycle from each EMG profile and normalized the EMG amplitude to the maximum computed over all cycles of a given participant and condition. EMG profiles were combined into an m × t matrix M, where m is the number of

recorded muscles and t is the number of time samples over the cycle (t = 200). NNMF algorithm finds a solution to the equation:

$$M \cong W \times P \qquad (4)$$

where M is a linear combination of temporal activation patterns P (n × t matrix, where n ≤ m is the number of selected patterns) and synergies weights W (m × n matrix). The W and P are estimated to minimize the root-mean-squared residual between M and W × P. The factorization uses an iterative method starting with random initial values for W and P. Because the root-mean-squared residual may have local minima, the best solution was selected out of 100 runs. Each run of the NNMF was carried out until a termination tolerance on change in size of the residual or in the elements of W and P set to 10^{-5}. We varied the number of basic patterns from 1 to 8 and retained for further analyses the smallest number of activation patterns, such that they accounted for ≥ 80% of the variance of EMG profiles when using Eq. 4.

CLUSTER ANALYSIS OF ACTIVATION PATTERNS. To identify similar activation patterns across cycles, all P (Eq. 4) extracted from single cycles of all subjects of each group and condition were pooled together and partitioned in k mutually exclusive patterns using the k-means algorithm (10). To minimize the possibility of misleading local minima, we performed 100 replications of the algorithm. We report the results obtained by including all cycles within predefined ranges of speeds to preserve relative homogeneity: 0.03-0.1 m/s for neonates and 0.05-0.2 m/s for infants. However, we also assessed potential effects of speed by considering different subsets of data, and we found no major differences. For kicking, we report the results for cycles corresponding to -100%÷100% FEU, but the results were similar when we considered cycles limited to 0%÷100% FEU.

Because the k-means method requires choosing the number of clusters as input, we determined the optimal number of clusters in the range 2 to 20 using the silhouette method (11). The centroid for each cluster was the point with minimum distance from all points in the cluster. As distance measure (in 200-dimensions space), we used $[1 - \cos\alpha_i]$, α_i being the angle between points (treated as vectors). With the silhouette method, the optimal number k of clusters was taken as that giving the largest average silhouette value (11). The silhouette value is a measure of how similar a given data point is to the other data points in its own cluster, when compared to data points belonging to different clusters. The silhouette S_i for the i-th point is defined as:

$$S_i = \frac{(b_i - a_i)}{\max(a_i, b_i)} \qquad (5)$$

where a_i is the average distance from the i-th point to the other points in the same cluster as i, and b_i is the minimum average distance from the i-th point to points in a different cluster, computed over all clusters. Silhouettes range from -1 to +1. A high silhouette indicates that i is well-matched to its own cluster, and poorly-matched to neighboring clusters. All activation patterns with S≤0.2 were considered unmatched and excluded from the cluster. For each subjects' group, the resulting

clusters of activation patterns were ordered chronologically, based on the timing of the main peak relative to the step or kick cycle. We also evaluated if clustering performed on the activation patterns was matched by a consistent clustering of the synergy weights W. To this end, for each cluster we calculated the silhouettes for the synergies weights of the corresponding activation patterns, and considered the weights with S>0.2 well clustered based on these patterns.
We independently verified the optimal number of clusters by using the Davies-Bouldin DB index (12).

$$DB = \frac{1}{k}\sum_{i=1}^{k} \max_{j \neq i} \{D_{ij}\} \tag{6}$$

D_{ij} is the within-to-between cluster distance ratio for the i-th and j-th clusters:

$$D_{ij} = \frac{\left(\bar{d}_i + \bar{d}_j\right)}{d_{ij}} \tag{7}$$

where $\bar{d}_i$ is the average Euclidean distance between each point in the i-th cluster and the centroid of the i-th cluster, and similarly for $\bar{d}_j$. $\overline{d_{ij}}$ is the distance between the centroids of the i-th and j-th clusters. For each group of subjects, we calculated DB for k = 1-8 and selected the optimal number of clusters such that adding one more cluster involved a decrement of DB≤0.05 (i.e., DB_k-$DB_{k+1} \leq 0.05$).

VALIDATION OF CLUSTER ANALYSIS. To test the hypothesis that the activation patterns we found in neonates were actually structured in clusters, we generated 100 different sets of randomized activation patterns. Randomization was performed according to one of two different procedures. In the first, the new activation patterns had random amplitude values, uniformly distributed between the 2.5 percentile and the 97.5 percentile of the amplitude values of the original patterns (13). In the second procedure, the new activation patterns were identical to the original ones but shifted along the cycle by random, uniformly distributed time-shifts. Next, we applied the k-means algorithm to each of 100 different random datasets generated by each procedure, using k=2 for stepping and k=4 for kicking (the optimal number of clusters determined experimentally for each condition, see *Results*). Finally, we compared the original clusters and the clusters obtained by randomization based on two metrics: the silhouettes and the normalized Hubert's gamma statistics (13). Comparisons were based on the 5-95 percentiles of each metric computed over the randomized activation patterns.

SIGNIFICANCE OF THE ACTIVATION PATTERNS. We further verified that the structure of the activation patterns found in neonates did not result from a bias intrinsic to the extraction method. To this end, we generated structure-less data with the same empirical amplitude distribution and smoothness of the experimental EMG data by randomly reshuffling all samples, independently for each muscle. The reshuffling procedure involved a random permutation of an index vector (running from 1 to the total number of samples; Matlab function randperm.m) for each muscle,

and then reordering the samples using the permuted index. We then constructed a simulated dataset with the same number of cycles and with the same duration of each cycle as the experimental data, and applied the cluster analysis described above.

CLUSTERING OF MUSCLE SYNERGIES. We performed cluster analysis of the synergies weights W (Eq. 4) for kicking and forward stepping in a manner similar to that used for the activation patterns.

SPATIAL DECOMPOSITION OF MUSCLE ACTIVITIES. We performed spatial decomposition using NNMF on concatenated EMG data of each neonate with at least 7 FEUs for kicking or 7 strides for stepping, and of all neonates together for stepping and kicking movements. We quantified the differences between the synergy structure of stepping and kicking in terms of the principal angles between the subspaces spanned by each set (14). We assessed the distribution of principal angles expected from different datasets sharing the same kicking and stepping synergies by extracting synergies from random partitions of the data. Each data set was divided randomly into two halves for 100 times. For each iteration, we calculated the principal angles between the synergies extracted from the two halves using singular value decomposition (14). We used these principal angles to construct randomly two subspaces (one for kicking and one for stepping) that were characterized by the same principal angles from a common base. Next, we used the distribution of the principal angles between these two subspaces over the 100 iterations to estimate the effect of noise and sampling variability on the differences between the subspaces identified by the synergies of kicking and stepping. Since the differences between synergy sets may also depend on their dimensions, we performed this analysis for all 9 possible combinations of kicking and stepping synergy sets with a number of synergies ranging from 2 to 4.

SIMILARITY OF ACTIVATION PATTERNS AND MUSCLE SYNERGIES. Similarity was computed as the scalar-product between each pair of vectors, after normalization to unit vectors (15). Similarity can range from 0 to 1, 1 corresponding to identical vectors.

RECONSTRUCTION OF MUSCLE ACTIVITIES. The ability of the activation patterns from neonate kicking to describe the EMGs of stepping in different age groups was evaluated by cross-fitting. To this end, we performed NNMF on concatenated EMG data of the kicking movements of 15 neonates with a full EMG dataset. Next, we fitted the EMGs of concatenated stepping separately for each group of children (neonates, g1-g6), using NNMF with constant patterns P derived from neonate kicking and updated synergies W (over 100 runs). This procedure was iterated 100 times, each time taking a random half of all steps of each group of children and computing the VAF of the reconstruction of the corresponding EMGs. In the Results, we report the median and 5-95 percentiles of VAF over all 100 iterations. For comparison, we performed a similar reconstruction of kicking EMGs using constant patterns P derived from 18 ground-stepping neonates and updated synergies W.

FRACTIONATION OF MUSCLE SYNERGIES OF NEONATE STEPPING**.** We tested the hypothesis that the synergies of preschoolers (g6) might result from the fractionation of the synergies of neonate ground-stepping. To this end, we modeled the muscle synergies of neonate ground-stepping as a linear combination of the synergies of preschoolers (15).

$$\bar{W}_k^n \approx \sum_{i=1}^{N^{g6}} f_i^k W_i^{g6} \quad (8)$$

Where $\bar{W}_k^n$ is the synergy vector of stepping neonates, $\bar{W}_i^{g6}$ the synergy vector of preschoolers, N^n the number of synergies of neonates, N^{g6} the number of synergies of preschoolers, coefficients $\bar{f}^k$ (≥ 0) specify how the kth neonate synergy may be fractionated into multiple synergies observed in the preschoolers, and k ranges from 1 to N^n. The coefficients $\bar{f}^k$ were identified using nonnegative least squares. Because each synergy of preschoolers could not result from simultaneous fractionation of more than one synergy of neonates, the least-squares optimization included the additional constraint that each synergy of preschoolers could contribute to the reconstruction of at most one synergy of neonates. We used bootstrapping with 100 iterations. At each iteration, we took a random half of all steps of both neonates and preschoolers, performed NNMF with fixed synergies, and computed for each neonate synergy the potential fractionation in preschoolers synergies. We carried out the same procedure also on random synergies, obtained by shuffling the experimental synergies of preschoolers. We considered fractionable the neonate synergies with scalar-product similarity of reconstruction > 0.75 and $f^k > 0.2$ (15).

Statistics

Descriptive statistics included means ± SD across all cycles of all participants of a given group. For data with skewed distributions, we report the median and 5-95 percentiles. One-way ANOVA test was used to evaluate the effect of speed on mean EMG activity. Circular statistics on directional data was used to characterize the mean CoA for each muscle (see above) and its variability across steps (circular SD). The Watson-Williams test was used for circular data (CoA across different speeds) to evaluate the effect of condition (stepping or kicking) in neonates. Post-hoc Bonferroni correction for multiple comparisons was used on circular data. We used the Rayleigh test for non-uniformity of circular data to check whether EMG waveforms or CoA samples were distributed uniformly around the cycle or had a common mean direction. Reported results were considered significant for $P < 0.05$.

References

1. N. Dominici *et al.*, Locomotor primitives in newborn babies and their development. *Science* 334,997-9 (2011).
2. Y.P. Ivanenko *et al.*, Changes in the spinal segmental motor output for stepping during development from infant to adult. *J. Neurosci.* 33, 3025-3036 (2013).
3. F. Sylos-Labini *et al.*, Foot placement characteristics and plantar pressure distribution patterns during stepping on ground in neonates. *Front. Physiol.* 8,784 (2017).
4. E. Thelen, D.M. Fisher, Newborn stepping: an explanation for a “disappearing” reflex. *Dev. Psychol.* 18, 760–775 (1982).
5. J.F. Yang, M.J. Stephens, R. Vishram, Infant stepping: a method to study the sensory control of human walking. *J. Physiol.* 507, 927-37 (1998).

6. H. Forssberg, Ontogeny of human locomotor control. I. Infant stepping, supported locomotion and transition to independent locomotion. *Exp. Brain Res.* 57, 480-93 (1985).
7. E. Domellöf, L. Rönnqvist, B. Hopkins, Functional asymmetries in the stepping response of the human newborn: a kinematic approach. *Exp Brain Res* 177, 324-335 (2007).
8. P. Berens, CircStat: A Matlab Toolbox for Circular Statistics. *J Stat Softw,* 31, 1-21 (2009)
9. D.D. Lee, H.S. Seung, Learning the parts of objects by non-negative matrix factorization. *Nature* 401,788–791 (1999).
10. P. Saltiel, K. Wyler-Duda, A. d'Avella, M.C. Tresch, E. Bizzi, Muscle synergies encoded within the spinal cord: evidence from focal intraspinal NMDA iontophoresis in the frog. *J. Neurophysiol.* 85,605-619 (2001).
11. P.J. Rousseeuw, Silhouettes: a graphical aid to the interpretation and validation of cluster analysis. *J. Comput. Appl. Math.* 20, 53-65 (1987).
12. D.L. Davies, D.W. Bouldin, A cluster separation measure. *IEEE Trans. Pattern Anal. Mach. Intell.* 1, 224-7 (1979).
13. S. Theodoridis, K. Koutroumbas, *Pattern Recognition*. (Academic Press, Burlington, MA, 2008).
14. G. H. Golub, C. F. Van Loan, *Matrix Computations*. 3rd Edition, Johns Hopkins University Press, Baltimore (1996).
15. V.C. Cheung *et al.*, Muscle synergy patterns as physiological markers of motor cortical damage. *Proc Natl Acad Sci U S A*. 109, 14652-6 (2012).

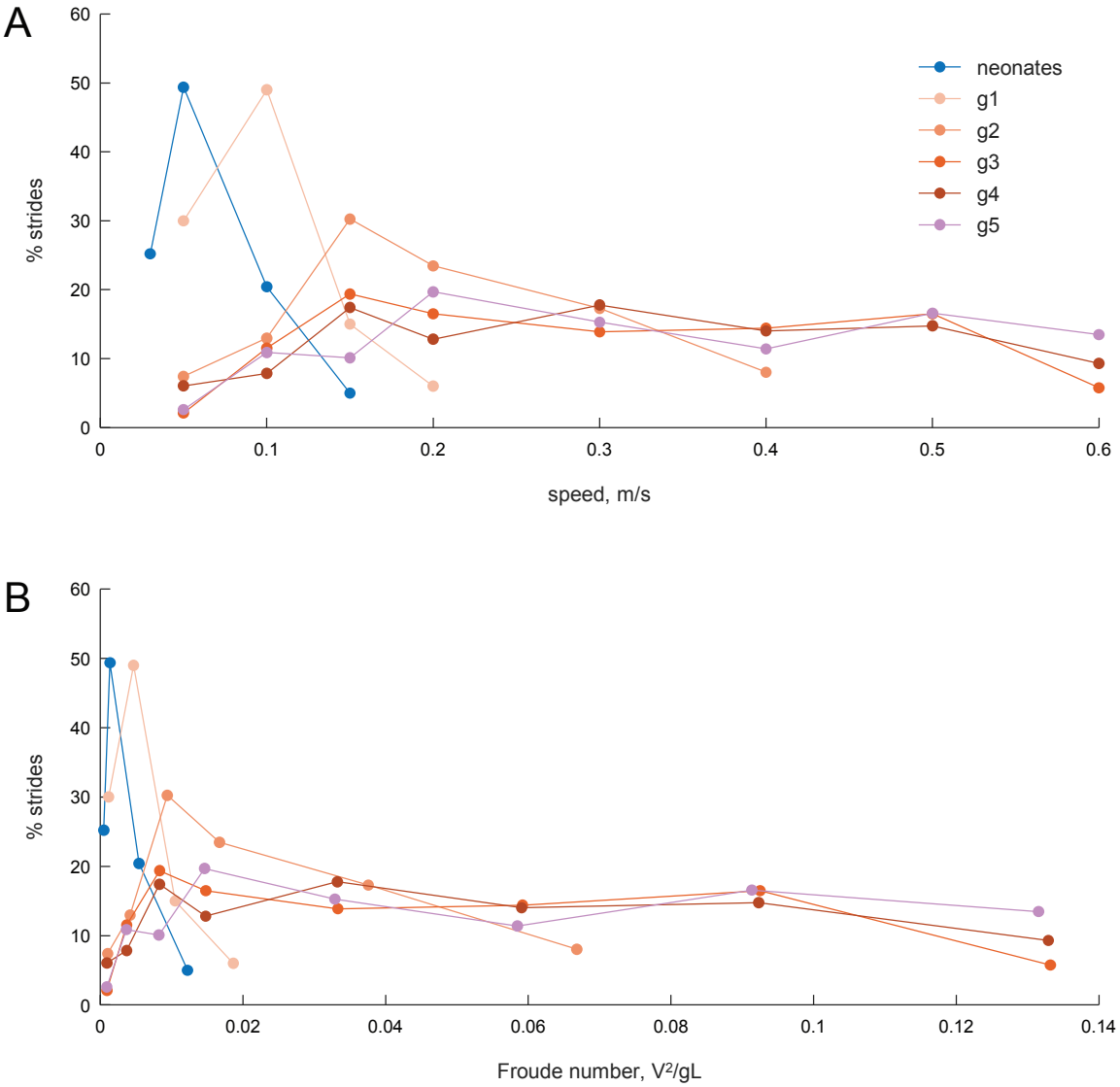
A
% strides
speed, m/s
neonates
g1
g2
g3
g4
g5
0
10
20
30
40
50
60
0
0.1
0.2
0.3
0.4
0.5
0.6
B
% strides
Froude number, V²/gL
0
10
20
30
40
50
60
0
0.02
0.04
0.06
0.08
0.1
0.12
0.14

Fig. S1. (A) Percent of strides as a function of treadmill speed. 480 strides from all neonates and 1857 strides from all infants stepping on treadmill are included. (B) Same results as in A plotted versus Froude numbers to take into account the different size of each child. V = treadmill speed, L = anatomical leg length (thigh + shank), g = gravitational acceleration (9.81 m/s^2). g1, 4-6 months infants; g2, 6-8 months; g3, 8-10 months; g4, 10-14 months; g5, toddlers, 12-15 months.

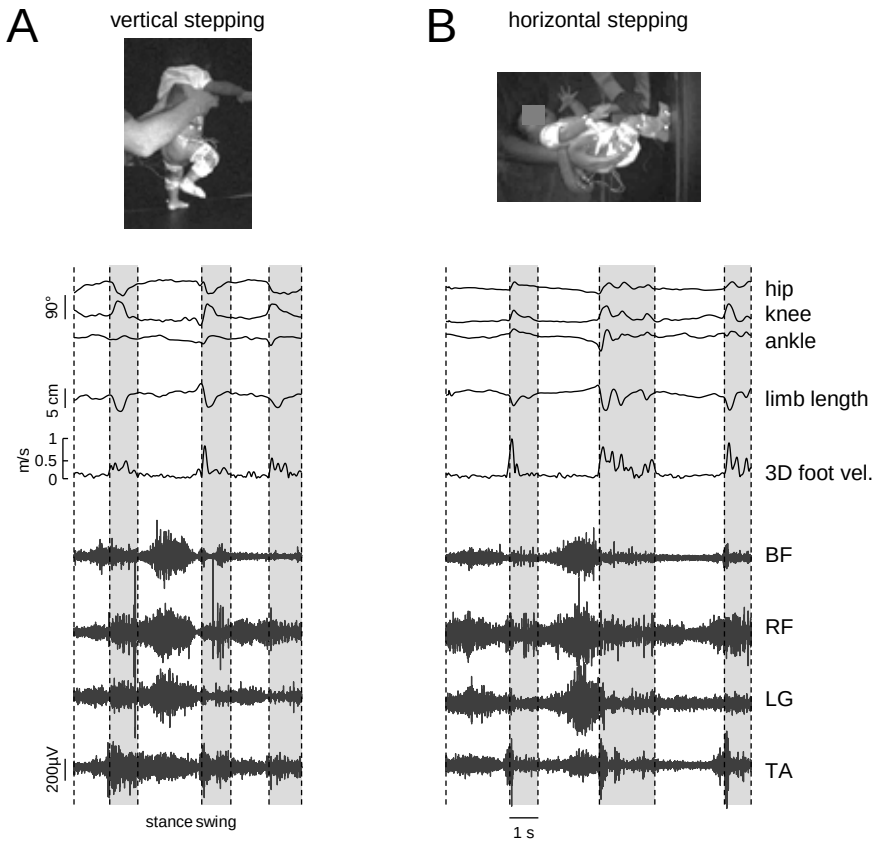
A
vertical stepping
B
horizontal stepping
90°
5 cm
m/s
1
0.5
0
200μV
stance swing
hip
knee
ankle
limb length
3D foot vel.
BF
RF
LG
TA
1 s

Fig. S2. Effect of posture on stepping. During the same experimental session, one neonate (3-day-old) stepped forward both when held in the standard vertical position (A) and when placed supine in a horizontal position (B). In the latter case, the treadmill was oriented perpendicular to the ground. BF, biceps femoris; RF, rectus femoris; LG, gastrocnemius lateralis; TA, tibialis anterior.

A

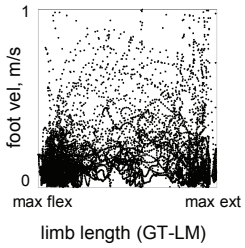
1
foot vel, m/s
0
max flex
max ext
limb length (GT-LM)

B

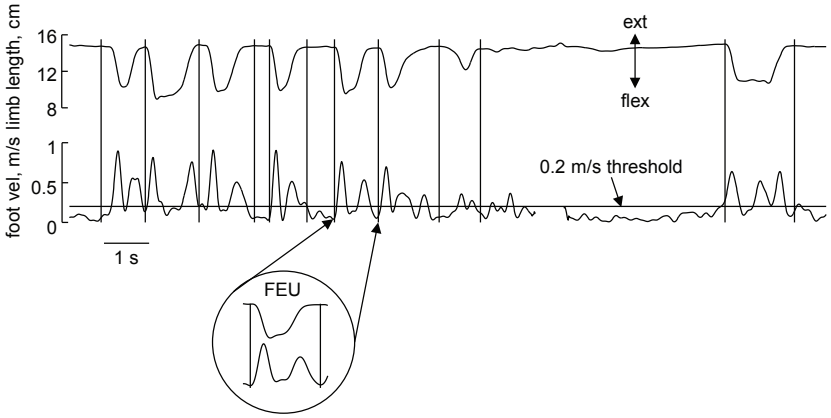
foot vel, m/s limb length, cm
16
12
8
1
0.5
0
ext
flex
0.2 m/s threshold
1 s
FEU

Fig. S3. Flexion-extension units (FEU) during spontaneous kicking. (A) Exemplary phase-plot of foot (5MT) velocity versus changes in effective limb length (GT-LM) over a ~2min trial in a two-day old neonate. Each data point corresponds to a single frame (100 Hz sampling rate). (B) Time course of changes in effective limb length and foot velocity during kicking. Onset and end of a FEU (vertical dashed lines) correspond to the maxima of limb length between two consecutive minima. We selected only FEUs in which the peak of foot velocity exceeded a threshold of 0.2 m/s.

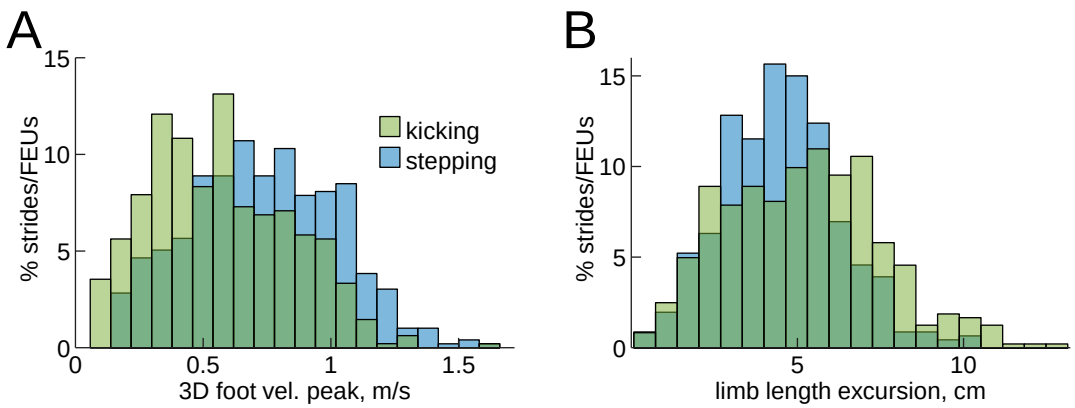
A
B
% strides/FEUs
kicking
stepping
3D foot vel. peak, m/s
limb length excursion, cm
0
5
10
15
0.5
1
1.5

Fig. S4. (A) Histogram of peak tangential velocity of the foot for kicking (n=480) and stepping (n=495) cycles in neonates. Tangential velocity was computed as $v = \sqrt{(\dot{x}^2 + \dot{y}^2 + \dot{z}^2)}$ where $\dot{x}$, $\dot{y}$ and $\dot{z}$ are the time-derivatives of the coordinates of the 5MT marker in the principal movement plane. (B) Histogram of changes of limb length during each cycle. Limb length was computed as the distance between GT and LM markers.

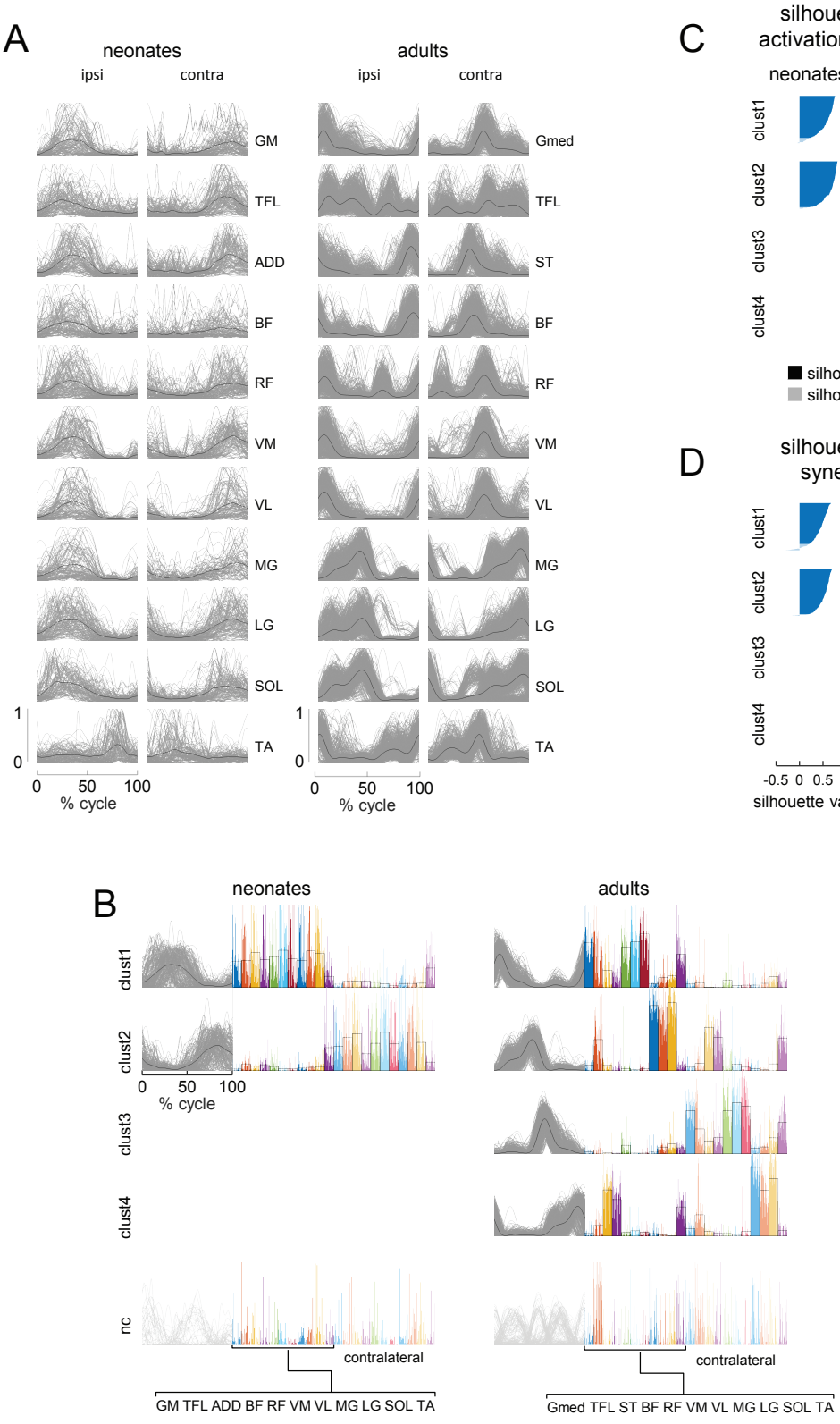
A
neonates
adults
ipsi
contra
GM
TFL
ADD
BF
RF
VM
VL
MG
LG
SOL
TA
Gmed
ST
1
0
0 50 100
% cycle
C
silhouettes of activation patterns
clust1
clust2
clust3
clust4
silhouette>0.2
silhouette≤0.2
D
silhouettes of synergies
-0.5 0 0.5 1
silhouette value
B
nc
contralateral
GM TFL ADD BF RF VM VL MG LG SOL TA
Gmed TFL ST BF RF VM VL MG LG SOL TA

Fig. S5. Cluster analysis of neuromuscular modules of 11 bilateral EMGs for stepping in neonates (n=10) and adults (n=16). (A) Rectified EMG profiles from single cycles of all subjects of each group in grey, average patterns in black. (B) Clusters of activation patterns (S>0.2) from single cycles of all subjects of each group in grey, average patterns in black. Synergies weights (S>0.2) for single cycles in color, average values as white bars. Bottom: Not-clustered (nc, S≤0.2) activation patterns (light grey) and associated weights. Silhouettes of activation patterns (B) and synergies weights (C) ranked in decreasing order for the single steps of panel A (below-threshold silhouettes in light color).

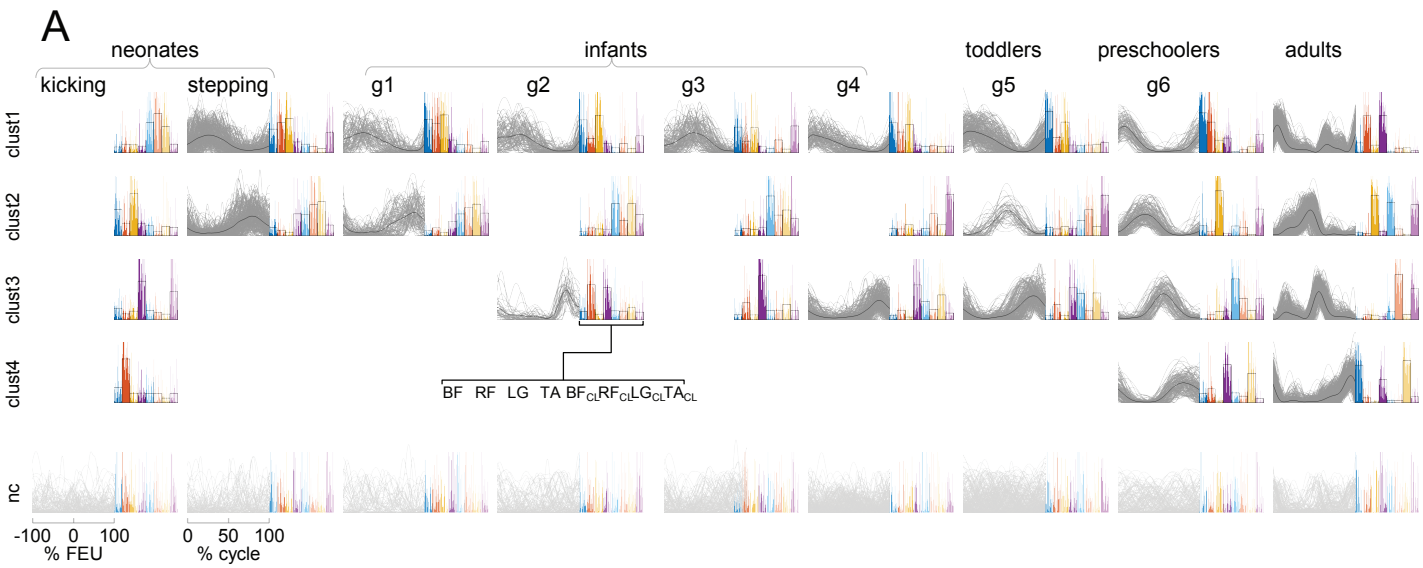
A
neonates
infants
toddlers
preschoolers
adults
kicking
stepping
g1
g2
g3
g4
g5
g6
clust1
clust2
clust3
clust4
nc
BF RF LG TA BF$_{CL}$ RF$_{CL}$ LG$_{CL}$ TA$_{CL}$
-100 0 100
% FEU
0 50 100
% cycle

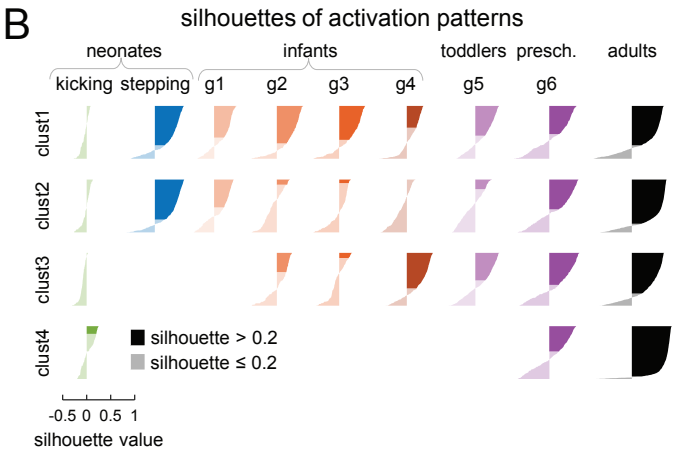
B
silhouettes of activation patterns
neonates
infants
toddlers
presch.
adults
kicking
stepping
g1
g2
g3
g4
g5
g6
clust1
clust2
clust3
clust4
silhouette > 0.2
silhouette ≤ 0.2
-0.5 0 0.5 1
silhouette value

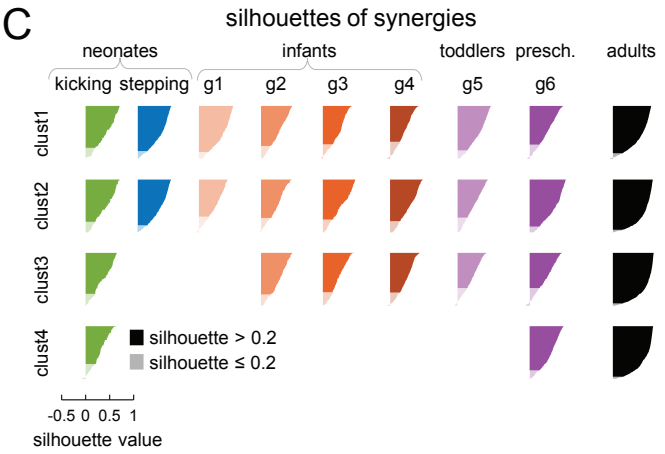
C
silhouettes of synergies
neonates
infants
toddlers
presch.
adults
kicking
stepping
g1
g2
g3
g4
g5
g6
clust1
clust2
clust3
clust4
silhouette > 0.2
silhouette ≤ 0.2
-0.5 0 0.5 1
silhouette value

Fig. S6. Clusterization of the neuromuscular modules of bilateral EMGs for neonate kicking and stepping based on muscle synergies in the same format as Figs. 3A-C. Patterns and synergies are plotted only if S>0.2 in >15% of cases.